Fermion- and Spin-Counting in Strongly Correlated Systems

Fermion- and Spin-Counting in Strongly Correlated Systems

Sibylle Braungardt[1], Aditi Sen(De)[1], Ujjwal Sen[1], Roy J. Glauber[2], and Maciej Lewenstein[*,1]
[1] *ICFO-Institut de Ciències Fotòniques, Mediterranean Technology Park, 08860 Castelldefels (Barcelona), Spain*
[2] *Lyman Laboratory, Physics Department, Harvard University, 02138 Cambridge, MA, U.S.A.*
[*] *ICREA Institució Catala de Ricerca i Estudis Avançats, 08010 Barcelona, Spain*

We apply the atom counting theory to strongly correlated Fermi systems and spin models, which can be realized with ultracold atoms. The counting distributions are typically sub-Poissonian and remain smooth at quantum phase transitions, but their moments exhibit critical behavior, and characterize quantum statistical properties of the system. Moreover, more detailed characterizations are obtained with experimentally feasible spatially resolved counting distributions.

I. INTRODUCTION

A. Particle- and spin-counting

Particle-wave duality is one of the most spectacular, and at the same time intriguing phenomena of quantum mechanics. Nevertheless, careful counting of particles, such as photons, in a given quantum mechanical state allows to fully reconstruct the wave nature and coherence properties of the state. The formulation of photon-counting theory in the frame of quantum electrodynamics [1] gave birth to modern quantum optics. Recent progress in physics of ultracold atoms made possible to develop and apply techniques of single atom counting to various systems. Since the pioneering experiments of Shimizu [2], spectacular measurements of Hanbury Brown - Twiss effect for bosons [3], and fermions [4] have been performed with ultra-cold meta-stable Helium atoms. Esslinger's group employed cavity quantum electrodynamics techniques to measure the pair correlation function in an atom laser beam outgoing from a trapped Bose condensate [5]. These new detection methods allow in principle to measure full atom-counting distributions with spatial resolution (by counting only atoms in a certain spatial region), and provide novel efficient ways of detection of strongly correlated systems [6].

Equally spectacular progress has been achieved in spin-counting, or in other words, measurements of total atomic spin for atoms with spin, or pseudo-spin degree of freedom. The idea of quantum non-demolition polarization spectroscopy (QNDPS), has been demonstrated in Ref. [7]. It employs the quantum Faraday effect: polarized light beam passed through the atomic sample, undergoes polarization rotation. Atomic fluctuations leave an imprint on the quantum fluctuations of the light, and vice versa. This idea was recently extended to ultra-cold spinor gases [8], where it can be used to detect, manipulate, and even engineer various states of such systems. Amazingly, this method allows also for a spatial resolution (when standing laser beams are employed) [9].

B. Main results

In this paper, we show how the atom counting techniques can be used to detect properties of strongly correlated systems. We concentrate, in particular, on the case of fermion and/or spin counting in one-dimensional (1D) optical lattices, that are equivalent, via Jordan-Wigner transformation [10], to 1D spin chains. The problem of spin counting for a local block of spins in the 1D Ising model in a transverse field has been considered in a beautiful work of Demler's group [11]. Our paper is in a sense complementary to Ref. [11]. First, we consider not only on the Ising model, but on the whole family of asymmetric XY models, characterized by the asymmetry parameter γ, in the transverse field h. Second, employing ideas of Ref. [9], we calculate not only the counting distribution for the total fermion number (total Z-spin component), but also for "effective" number, corresponding to certain spatial Fourier components of the fermion density. While for the considered family of models, counting distributions are always smooth, their cumulants exhibit critical behavior, evident even for small detection efficiencies. The distributions are always sub-Poissonian, but the sub-Poissonian character changes, as we sweep h from 0 to ∞. For small (large) γ, the $h = 0$ ($h = \infty$) distribution is always the narrower (broader) one. Through the paper, we use an elegant generalization of the photon-counting theory to fermions, derived by Cahill and Glauber within the formalism of Grassmann variables [12]. For the cases we consider, we obtain analytic expressions for the counting distribution in terms of simple recursion relations.

The paper is organized as follows. In Sec. II, we briefly describe the models of the 1D optical lattice that we consider, and the Jordan-Wigner transformation that can be used to diagonalize them. In the next section (Sec. III), we derive the counting statistics of fermions in the systems described by these models; in particular, we discuss them for the Ising model (Subsec. III D), and more generally for the asymmetric XY model (Subsec. III E). In Subsec. III F, we consider the means and variances of the counting distributions: We derive recurrence relations that allow for easy calculation of these moments for an arbitrary number of particles in the system. We discuss also the generalization of our method to the case

of Fourier components of the total spin in Subsec. III H. Finally, we summarize our results in Sec. IV.

II. FERMI GAS IN AN 1D OPTICAL LATTICE

A. 1D Fermi gases

Let us consider a family of models describing an one-dimensional Fermi gas in an optical lattice, described by the Hamiltonian

$$H = -\frac{J}{2}\sum_{j=0}^{N-1}\left[c_j^\dagger c_{j+1} + \gamma c_j^\dagger c_{j+1}^\dagger + \text{h.c.} - 2g c_j^\dagger c_j\right] + \frac{1}{2}Ng, \tag{1}$$

where $J/2$ is the energy associated to fermion tunneling, $g = h/J$, and N is the number of sites. One way to realize such Hamiltonian with ultracold atoms is to use a Fermi-Bose mixture in the strong coupling limit. In this limit, the low energy physics is well described by fermionic composites theory [13], in which fermions form composite objects with $0, 1, \ldots$ bosons, or bosonic holes repectively. The fermionic composites undergo tunneling and interact via nearest neighbor interactions, which may be repulsive or attractive, weak or strong, depending on the original parameters of the system, such as scattering lengths, etc. In the case of weak attractive interactions, the system undergoes, at zero temperature, a transition into a "p-wave" superfluid, described well by the Bardeen-Cooper-Schrieffer (BCS) theory, corresponding exactly to the Hamiltonian (1).

B. 1D spin chains

Using Jordan-Wigner transformation [10], one can transform the Hamiltonian (1) into the one of a 1D asymmetric XY spin chain in the transverse magnetic field h,

$$H_{xy} = J\sum_{j=0}^{N-1}\left[(1+\gamma)S_j^x S_{j+1}^x + (1-\gamma)S_j^y S_{j+1}^y - \frac{h}{J}S_j^z\right], \tag{2}$$

where $S_j^\alpha = \frac{1}{2}\sigma_j^\alpha$ are the spin 1/2 operators at site j, proportional to Pauli matrices. The special cases $\gamma = 0$ (i.e. the so called symmetric XY, or XX limit) and $\gamma = \pm 1$ can be realized with single species bosons in the hard core (i.e. strongly repulsive) bosons limit [10, 14], or in a chain of double well sites filled with bosons interacting via weak dipolar forces [15], respectively. In general, one should use a two component Bose-Bose and Fermi-Fermi mixture, which, in the strong coupling limit, and in the Mott insulator state with one atom per site, is described by an asymmetric (XXZ) Heisenberg model (cf. [16]) in the Z oriented field. By appropriate tuning of the scattering lengths via Feshbach resonances, one can set the $S_{j+1}^z S_j^z$ coupling to zero, i.e. achieve the XX model in the transverse field. In order to introduce the asymmetry γ, one should additionally introduce tunneling assisted with a laser or microwave induced double spin flip. For this aim, one should make use of the resonance between on-site two atom "up-up" and "down-down" states, without disturbing "up-down" configurations.

C. Jordan-Wigner transformation

As it is well known, Jordan-Wigner transformation works for open chains, and in particular for an infinite chain. We will nevertheless assume periodic boundary conditions to solve the fermion model (1) using Fourier and Bogoliubov transformations (see e.g. [17]). For large N, such precedure gives the right leading behaviour. We define Fourier transformed operators as

$$c_j^\dagger = \sum_{k=0}^{N-1}\exp(-ij\Phi_k)a_k^\dagger, \tag{3}$$

and

$$c_j = \sum_{k=0}^{N-1}\exp(ij\Phi_k)a_k, \tag{4}$$

where $\Phi_k = 2\pi k/N$. We perform then the Bogoliubov transforms

$$a_k = u_k d_k - iv_k d_{N-k}^\dagger, \quad a_k^\dagger = u_k d_k^\dagger + iv_k d_{N-k}, \tag{5}$$

where u_k, v_k are real numbers satisfying

$$\begin{aligned} &u_k^2 + v_k^2 = 1, \\ &u_{N-k} = u_k \quad \text{and} \quad v_{N-k} = -v_k, \end{aligned} \tag{6}$$

so that we can write

$$u_k = \cos\frac{\theta}{2}, \text{ and } v_k = \sin\frac{\theta}{2}. \tag{7}$$

When

$$\tan\theta = \frac{\gamma\sin\Phi_k}{\cos\Phi_k - g}, \tag{8}$$

the Hamiltonian reduces then to the noninteracting fermions Hamiltonian,

$$H = \frac{1}{2}\sum_{k=0}^{N-1}\epsilon_k d_k^\dagger d_k, \tag{9}$$

with

$$\epsilon_k = 2\sqrt{(\cos\Phi_k - g)^2 + \gamma^2\sin^2\Phi_k}. \tag{10}$$

The ground state is thus the vacuum of the d_k operators. For $\gamma > 0$ the spectrum is everywhere gapped, except at the critical point $g_c = 1$. For $\gamma = 0$, d_k's coincide with a_k's or $a_k^\dagger$'s, and the ground state is a Fermi sea. For $-1 \le g \le 1$ the spectrum is then gapless and the system critical. Note that the number of original fermions $\hat{N}_f = \sum_{i=0}^{N-1} c_i^\dagger c_i$, as well as the the total Z-component of the spin, $\hat{S}^z = \sum_{i=0}^{N-1} S_i^z = \hat{N}_f - 1/2$ are not conserved, except at $\gamma = 0$.

III. FERMION COUNTING STATISTICS

A. Fermion counting distributions

Let us now turn to counting procedures. For the case of fermions, one should think about the analogue approach as one used in the experiments on metastable Helium. For spins, one could use directly QNDPS to measure the distribution of $\hat{S}_z$, or even its spatially resolved version [9]. An alternative way would be to switch off the Hamiltonian (2) (by switching off lasers), and induce spontaneous Raman transition from the state "up" to some side level. Counting of spontaneously emitted photons would correspond then to counting of "up" spins"

Mathematically, as known for photons [1], and generalized by Cahill and Glauber for fermions [12], the probability of detecting m photons in a given interval of time can be expressed as the mth derivative with respect to a parameter λ of the generating function $\mathcal{Q}(\lambda)$ as

$$p(m) = \frac{(-1)^m}{m!}\frac{d^m}{d\lambda^m}\mathcal{Q}\Big|_{\lambda=1}, \tag{11}$$

where $\mathcal{Q}(\lambda)$ is the expectation value of a normally ordered exponential $\mathcal{Q}(\lambda) = \mathrm{Tr}(\rho : e^{-\lambda\mathcal{I}} :)$. The operator $\mathcal{I}$ is a space-time integral of the product of the positive-frequency and negative-frequency parts of the quantum fields describing particles to be counted. The mean values of normally ordered products can be calculated in a particularly convenient and elegant way using the Grassmann variables formalism, introduced in [12]. In the case of counting the total number of particles, we have $\mathcal{I} = \kappa\sum_{j=0}^{N-1} c_j^\dagger c_j = \kappa\sum_{j=0}^{N-1}\sigma_j^\dagger\sigma_j = \kappa\sum_{k=0}^{N-1} a_k^\dagger a_k$, where $\kappa = 1-\exp(-\zeta t)$, while $0 \le \zeta \le 1$ is the detector efficiency, and t is the exposure time. For the spatially resolved QNDPS, $\mathcal{I} = \kappa\sum_{j=0}^{N-1}\sigma_j^\dagger\sigma_j\cos(\mathbf{k}_L\mathbf{r}_j)$, where $\mathbf{k}_L$ is the wave vector of the standing wave used for detection, and $\mathbf{r}_j$ is the position of the j-th site.

For counting the total number of particles, the generating function $\mathcal{Q}(\lambda)$ can be written as

$$\mathcal{Q}(\lambda) = \mathrm{Tr}(\rho : e^{-\lambda\kappa\sum_{k=0}^{N-1} a_k^\dagger a_k} :). \tag{12}$$

The operators $a_k^\dagger a_k$ commute for different k, so that the expression for $\mathcal{Q}$ can be rewritten as

$$\begin{aligned}
\mathcal{Q}(\lambda) &= \mathrm{Tr}(\rho : \prod_{k=0}^{N-1}(e^{-\lambda\kappa a_k^\dagger a_k}) :) \\
&= \mathrm{Tr}(\rho : \prod_{k=0}^{N-1}(1-\lambda\kappa a_k^\dagger a_k + \lambda^2\kappa^2 a_k^\dagger a_k a_k^\dagger a_k + ...) :) \\
&= \mathrm{Tr}(\rho\prod_{k=0}^{N-1}(1-\lambda\kappa a_k^\dagger a_k)) \\
&= \mathrm{Tr}(\rho\prod_{k=1}^{N/2}(1-\lambda\kappa a_k^\dagger a_k)(1-\lambda\kappa a_{N-k}^\dagger a_{N-k})),
\end{aligned}$$

as : $a_k^\dagger a_k a_k^\dagger a_k := a_k^\dagger a_k^\dagger a_k a_k = 0$, etc.

The terms $a_k^\dagger a_k$ and $a_{N-k}^\dagger a_{N-k}$ can then be expressed in terms of the d fermions:

$$\begin{aligned}
a_k^\dagger a_k &= (u_k d_k^\dagger + iv_k d_{N-k})(u_k d_k - iv_k d_{N-k}^\dagger), \\
a_{N-k}^\dagger a_{N-k} &= (u_k d_{N-k}^\dagger - iv_k d_k)(u_k d_{N-k} + iv_k d_k^\dagger).
\end{aligned}$$

B. Generating function for the ground state

We consider the counting statistics of the c fermions in the ground state of the Hamiltonian, i.e. *in the vacuum state of d fermions*.

The trace in the generating function can be now easily calculated by the formalism of Grassmann variables [12]. The P representation for the density operator ρ is

$$\rho = \int d^2\vec{\alpha}P(\vec{\alpha})|\vec{\alpha}\rangle\langle\vec{\alpha}|, \tag{13}$$

where $|\vec{\alpha}\rangle$ are the fermionic coherent states, as defined in [12]. Using the P representation, the mean values of normally ordered products of d-fermions can then be calculated as

$$\begin{aligned}
\mathrm{Tr}(\rho d_k^{\dagger n} d_l^m) &= \int d^2\vec{\alpha}P(\vec{\alpha})\langle\vec{\alpha}|d_k^{\dagger n}d_l^m|\vec{\alpha}\rangle \\
&= \int d^2\vec{\alpha}P(\vec{\alpha})\alpha_k^{*n}\alpha_l^m,
\end{aligned} \tag{14}$$

where the α_i are Grassmann variables, and are defined by the eigen-equation $d|\alpha_i\rangle = \alpha_i|\alpha_i\rangle$. For the vacuum state of the d-fermions,

$$\rho = |0...0\rangle\langle 0...0|, \tag{15}$$

the P-function is given by

$$P(\alpha) = \int d^2\vec{\xi}\exp\left(\sum_i(\alpha_i\xi_i^* - \xi_i\alpha_i^*)\right) = \delta(\vec{\alpha}). \tag{16}$$

Evaluating Eq. (14) using Eq. (16), we get the relations

$$\mathrm{Tr}(\rho d_k^{\dagger n} d_l^m) = \int d^2\vec{\alpha}\prod_i(\alpha_i^*)^{n_i}\alpha_i^{m_i}\delta(\vec{\alpha}) = 0, \tag{17}$$

and

$$\mathrm{Tr}(\rho) = \int d^2\vec{\alpha}\delta(\vec{\alpha}) = 1. \tag{18}$$

The relevant remaining terms in the product $(1-\lambda\kappa a_k^\dagger a_k)(1-\lambda\kappa a_{N-k}^\dagger a_{N-k})$ in the generating function are thus

$$\begin{aligned}
&1 - \lambda\kappa v_k^2 d_{N-k}d_{N-k}^\dagger - \lambda\kappa v_k^2 d_k d_k^\dagger \\
&+\lambda^2\kappa^2 v_k^4 d_{N-k}d_{N-k}^\dagger d_k d_k^\dagger - \lambda^2\kappa^2 v_k^2 u_k^2 d_{N-k}d_k d_{N-k}^\dagger d_k^\dagger
\end{aligned}$$

Elementary calculations using the relations (17) and (18) yield

$$\mathcal{Q}(\lambda) = \prod_{k=1}^{N/2} \left(1 - 2\lambda\kappa v_k^2 + \lambda^2\kappa^2 v_k^2\right). \tag{19}$$

At this point it is convenient to introduce the distribution function $p(m, M)$ of counting m particles for M pairs of modes. It is given by the same expression as before, but with the product in Eq. (19) limited to $M/2$ terms.

C. Counting statistics

The counting distribution is calculated from the generating function by the relation in Eq. (11). We use the generalized Leibniz rule,

$$\frac{d^m}{d\lambda^m} \prod_{k=1}^{N} f_k(\lambda) = \sum_{n_1+\ldots+n_N=n} \binom{n}{n_1, n_2, ..., n_N} \prod_{k=1}^{N} \frac{d^{n_k}}{d\lambda^{n_k}} f_k(\lambda),$$

where the generalized Newton's symbol is given by

$$\binom{n}{n_1, n_2, ..., n_N} = \frac{n!}{n_1! n_2! ... n_N!},$$

to derive a recurrence relation, to calculate the distribution for $(M + 1)$ modes, given the distribution for M modes.

The distribution function $p(m, M)$ for M modes is given by

$$p(m, M) = \frac{(-1)^m}{m!} \frac{d^m}{d\lambda^m} \mathcal{Q}\Big|_{\lambda=1} = \frac{(-1)^m}{m!} \sum \frac{m!}{l_1! l_2! ... l_N!} \prod_{j=1}^{M/2} \frac{d^{l_j}}{d\lambda^{l_j}} (1 + A\lambda + B\lambda^2), \tag{20}$$

where the summations run over $l_1, \ldots, l_M$ such that $l_1 + \cdots + l_M = m$, where $l_j = 0$, 1, or 2, for $j = 1, \ldots, M$.

We can now derive the recursive relation

$$p(m, M + 1) = \sum_{i=0}^{2} \mathcal{P}_i p(m - i, M) \tag{21}$$

where

$$\begin{aligned} \mathcal{P}_0 &= 1 - 2\kappa v_{M+1}^2 + \kappa^2 v_{M+1}^2, \\ \mathcal{P}_1 &= 2\kappa v_{M+1}^2 - 2\kappa^2 v_{M+1}^2, \\ \mathcal{P}_2 &= 1 - \mathcal{P}_0 - \mathcal{P}_1 \end{aligned} \tag{22}$$

are the probabilities of detecting 0,1, or 2 particles in the modes $M + 1$ and $N - M - 1$. Therefore, starting from $p(0, 1) = 1 - 2\kappa v_1^2 + \kappa^2 v_1^2$, $p(1, 1) = 4\kappa v_1^2$ and $p(2, 1) = \kappa v_1^2$, we can use the recurrence relation (21) to calculate the counting distribution for an arbitrary number of modes.

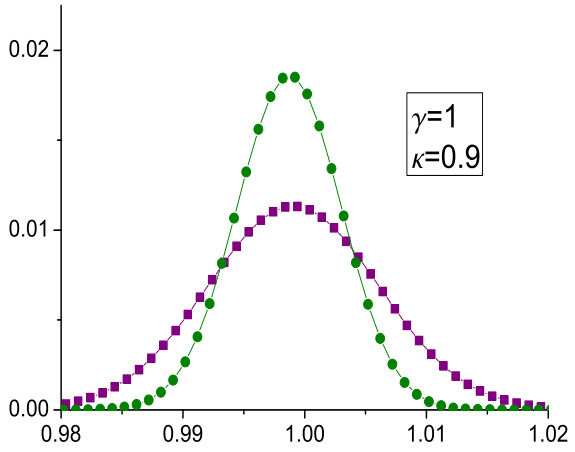

FIG. 1: Counting statistics of the transverse Ising model. The horizontal axis is $(m - \bar{m})/N + 1$. The vertical axis is of the corresponding probability. The curve with purple squares is for $h/J = 0.01$, while the one with green circles is for $h/J = 10$. The QPT of this model is at $h/J = 1$. Both the distributions are sub-Poissonian. However, the counting distribution becomes much narrower in the case when $h/J > 1$ than the situation when $h/J < 1$. In this case, we have taken the efficiency κ as 0.9.

Let us turn now to our results and discuss the counting statistics for different values of γ. In the figures that we plot below (except in Fig. 6 in Subsec. III G), we choose a value of the total number of modes, N, such that the corresponding quantities (distribution, mean, variance, etc.) have already converged. In the cases that we consider, such convergence occurs for $N \approx 300$.

D. Transverse Ising model

The counting distributions for the transverse Ising model (transverse XY model with $\gamma = 1$) for two exemplary values of the field parameter $g = h/J$ are shown in Fig. 1. The Ising model has a quantum phase transtition at $g = 1$ [10], and one exemplary value of g is chosen below the QPT, and the other above it. The difference in behavior is clearly seen. ($\overline{m}$ and var denote the mean and variance of the distribution, respectively.) Below, it will be more clearly revealed by looking at the mean and the variance of the distribution.

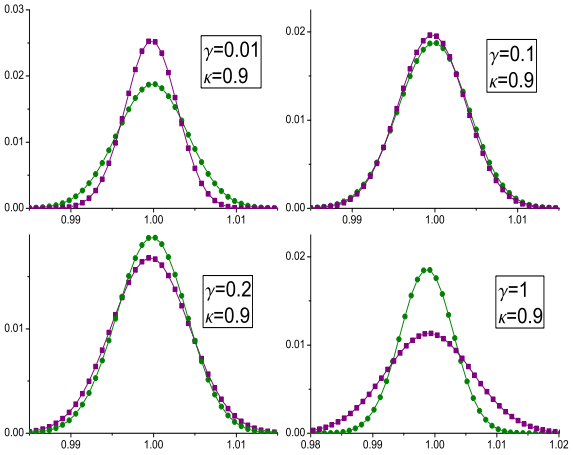

FIG. 2: Fermion counting distribution as a function of $(m - \overline{m})/N + 1$ (horizontal axis) for $\kappa = 0.9$, and for the indicated values of γ. Purple squares correspond to $h/J \to 0$, while green circles to $h/J \to \infty$. The transition anisotropy is here at $\gamma \approx 0.1$.

E. Transverse XY model: "Transition anisotropy"

In Fig. 2, we plot counting distributions as a function of $(m - \overline{m})/N + 1$ for four values of γ, for a fixed value of the efficiency $\kappa = 0.9$, and for two extreme values of g: $g \to 0$ and $g \to \infty$. Note that all the distributions presented in Fig. 2 are smooth and their widths ($\simeq \sqrt{var}/N$) are of order of 0.01. Since, as we argue below, $\overline{m} \simeq \kappa N$, all the distributions are sub- Poissonian, because $var \leq \bar{m}$, despite the finite detection efficiency. For $\gamma \to 0$, the distribution for $g \to 0$ is narrower than that for $g \to \infty$. This tendency is inverted in the Ising model, when the distribution for $g \to 0$ has a *larger* variance than the one for $g \to \infty$. At, what we call, *transition anisotropy* $\gamma \approx 0.1$, the distributions for $g \to 0$ and $g \to \infty$ practically coincide.

This transition anisotropy depends on the efficiency κ, and it moves to $\gamma \to 0$, as $\kappa \to 1$. This indicates that the probability distribution of counting can distinguish the two universality classes (the XX, with $\gamma = 0$, and the Ising, with $\gamma > 0$) among the XY models on a chain. In the limit of $\kappa \to 1-$, only the model with $\gamma \to 0$ has lower variance for $g \to 0$ as compared to $g \to \infty$, while all the other XY models (with $\gamma \neq 0$) have the opposite behavior.

F. Recurrence relations for mean and variance

In order to understand the properties of counting distributions better, we look at the mean and variance, which can be calculated from the following recurrences:

$$\overline{m_{M+1}} = \overline{m_M} + 2\kappa v_{M+1}^2, \tag{23}$$

$$var_{M+1} = \overline{m_{M+1}^2} - \overline{m_{M+1}}^2$$

$$= var_M + 4\kappa^2 v_{M+1}^2 (1 - v_{M+1}^2) \tag{24}$$

Since $\overline{m_1}$ and var_1 can be trivially calculated, the mean and variance can be obtained by these relations for an arbitrary number of modes. The recurrences imply that the mean $\overline{m_N} \leq \kappa N$; we find typical value of $\overline{m_N}$ indeed of order of κN. On the other hand, the variance $var_N \leq \kappa^2 N$. Both quantities show singular behavior in the thermodynamical limit at criticality. In particular, for the transverse Ising model ($\gamma = 1$), near the critical point $g = g_c \equiv 1$, the mean $\overline{m}$ can be written in terms of elliptic integrals of first and second kind, and can be expressed as [18]

$$\overline{m} \approx -\frac{1}{2\pi}(g - g_c) \ln|g - g_c| - \frac{1}{\pi},$$

so that

$$d\overline{m}/dg \approx -(\ln|g - g_c| + 1)/2\pi.$$

Since all models with $\gamma \neq 0$ belong to the same universality class, they all present the same singular behavior [10]. This is contrasted with the case of XX model, which belongs to a different universality class. The singular behavior is clearly seen in the plots of $\overline{m}/N$ and var/N obtained for finite $N \simeq 300$ and ideal $\kappa = 1$ (see Fig. 3). For finite values of γ, the variance shows a jump in the first derivative, while the first derivative of the mean tends to "infinity" at g_c. This behavior is better seen, when one plots directly the derivatives of $\overline{m}$ and var (see Fig. 4). This behavior changes drastically as $\gamma \to 0$. The variance tends then to zero (in the symmetric XX model the particle number is conserved), and the mean has a diverging derivative for $g < g_c$, and is constant for $g > g_c$. Amazingly, although finite detector efficiency obviously smoothes out the curves, the signatures of the singularities are clearly visible even for $\kappa = 0.5$ (see Fig. 5). A clear change of behavior of the curves is visible even at $\kappa = 0.1$! Note, that in all considered cases so far, the variance $var/N < \overline{m}/N$, i.e. all distributions are sub-Poissonian. Note, however, that going from antiferromagnetic to the *ferromagnetic* case, does not affect the variance, but replaces $\overline{m}/N \to (1/2 - \overline{m}/N)$. In that case we do observe a transition from sub-Poissonian behavior at small $g < g_t$, to (weakly) super-Poissonian for $g > g_t$; the value of g_t tend to g_c from below as $\gamma \to 0$.

G. Even versus odd splitting

The Bogoliubov transformation used to solve the considered models can be regarded as a "squeezing" or "pairing" transformation. The ground state that we investigated is analogous to BCS states of semiconductors, i.e.

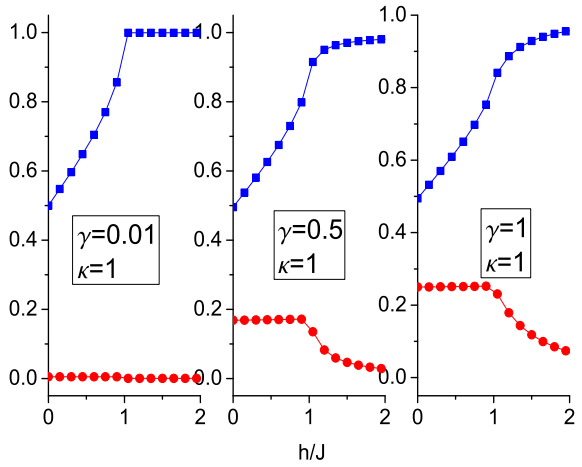

FIG. 3: Mean $\overline{m}/N$ (blue squares) and variance var/N (red circles) of the fermion counting distribution as a function of $g = h/J$ for $\kappa = 1$, and indicated values of γ.

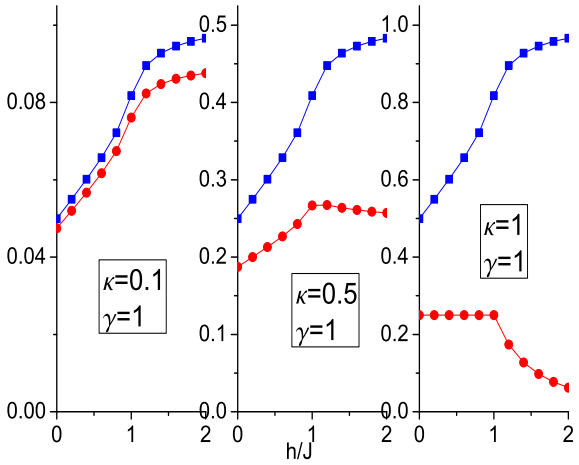

FIG. 5: Mean $\overline{m}/N$ (blue squares) and variance var/N (red circles) of the fermion counting distribution as a function of $g = h/J$ for $\gamma = 1$, and indicated values of κ.

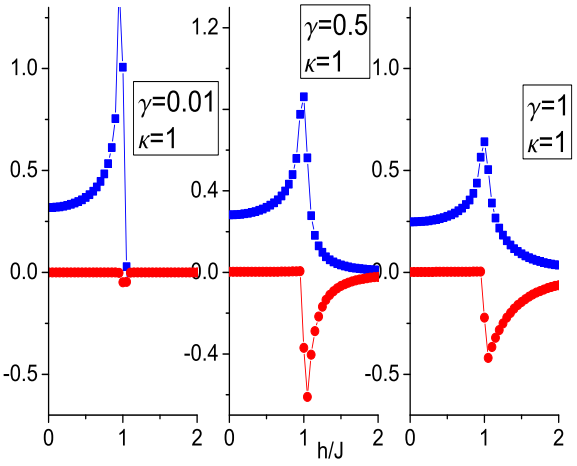

FIG. 4: The derivatives of the means and variances are plotted against the transverse field h/J (horizontal axis), for $\gamma = 0.01$, $\gamma = 0.5$, and $\gamma = 1$. Blue squares denote the derivatives of the means, while red circles denote the derivatives of the variances, in the respective cases. Also, $\kappa = 1$. The QPTs of all the models at $g = 1$ are clearly visible.

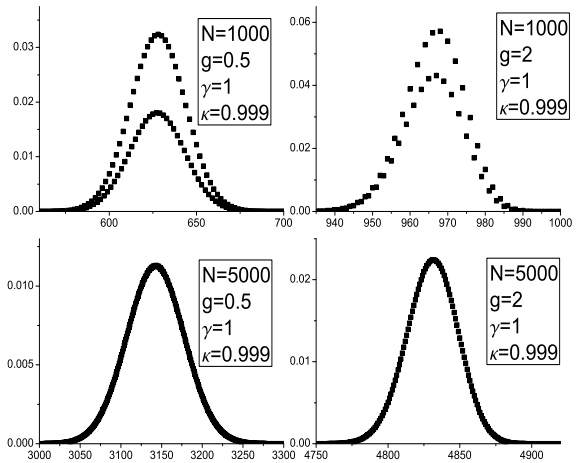

FIG. 6: Even versus odd splitting for $\kappa = 0.999$ in the Ising model. For N=1000 the probability distribution splits up, whereas for N=4000 there is no splitting.

they involve fermion (Cooper-like) pairs. Thus, in the ideal case of $\kappa = 1$, the counting distributions are exactly zero for odd numbers of particles. In practice, for finite values of N and $\kappa < 1$, the distributions oscillate between larger values for even, and small for odd number of counts. This behavior is very strongly affected by $\kappa < 1$, since at finite efficiency, one may easily miss single atoms from the Cooper pairs, and obtain odd counts.

In effect, for a given value of N, the even-odd asymmetry is visible only for κ close enough to 1. Similarly, the even-odd asymmetry is strongly affected by the finite size effects - for a given value of $\kappa < 1$ it is visible only for N small enough (see Fig. 6).

H. Counting spatial Fourier components of the fermion density

Finally, let us point out that the methods proposed in [9] allow for measurements of various kinds of Fourier components of the total spin; in terms of particle counting, these methods allow for instance to count particles in every second, every third site, etc. Our theory is easily generalized to such situations.

In the case when we count every second c fermion, we have to express $b^\dagger_{2j}b_{2j} = c^\dagger_{2j}c_{2j}$ in terms of the d fermions. As before, as a first step we do the Fourier transform:

$$\begin{aligned} c^\dagger_{2j} &= \sum_{k=0}^{N-1} \exp(-2ij\Phi_k) a^\dagger_k, \\ c_{2j} &= \sum_{k=0}^{N-1} \exp(+2ij\Phi_k) a_k. \end{aligned} \tag{25}$$

The expression $\sum_{j=0}^{N/2-1} c^\dagger_{2j}c_{2j} = \frac{1}{2}\sum_{j=0}^{N-1} c^\dagger_{2j}c_{2j}$ can thus be written as

$$\sum_{j=0}^{N/2-1} c^\dagger_{2j}c_{2j} = \frac{1}{2}\sum_{k,k'} \frac{1-\exp\left(4\pi i(k-k')\right)}{1-\exp\left(4\pi i(k-k')/N\right)} a^\dagger_k a_{k'}, \tag{26}$$

which is non vanishing for $k-k'=0$ or $|k-k'| = \frac{N}{2}$. Finally

$$\begin{aligned} &\sum_{j=0}^{N/2-1} c^\dagger_{2j}c_{2j} \\ &= \frac{1}{2}\sum_{j=0}^{N/2-1} a^\dagger_k a_k + a^\dagger_{k+N/2}a_{k+N/2} + a^\dagger_k a_{k+N/2} + a_{k+N/2}a_k \\ &= \frac{1}{2}\sum_{j=0}^{N/2-1} (a^\dagger_k + a^\dagger_{k+N/2})(a_k + a_{k+N/2}). \end{aligned} \tag{27}$$

We can now calculate $\mathcal{Q}(\lambda)$ as follows:

$$\begin{aligned} \mathcal{Q}(\lambda) &= \mathrm{Tr}(\rho : \prod_{k=0}^{N/2-1} e^{-\frac{1}{2}\lambda\kappa(a^\dagger_k + a^\dagger_{N/2+k})(a_k + a_{N/2+k})} :) \\ &= \prod_{k=0}^{N/2-1} \Big(1 - \frac{1}{2}\lambda\kappa(a^\dagger_k + a^\dagger_{N/2+k})(a_k + a_{N/2+k})\Big) \\ &= \prod_{k=1}^{N/4} \Big((1 - \frac{1}{2}\lambda\kappa(a^\dagger_k + a^\dagger_{N/2+k})(a_k + a_{N/2+k})) \\ &\times (1 - \frac{1}{2}\lambda\kappa(a^\dagger_{N-k} + a^\dagger_{N/2-k})(a_{N-k} + a_{N/2-k}))\Big). \end{aligned} \tag{28}$$

After performing the Bogoliubov transform, and keeping the relevant terms for the vacuum state of the d fermions, the generating function $\mathcal{Q}$ is given by

$$\mathcal{Q}(\lambda) = \prod_{k=1}^{N/4} \Big(1 - 2\lambda\kappa v_k^2 + \lambda^2\kappa^2 v_k^2\Big), \tag{29}$$

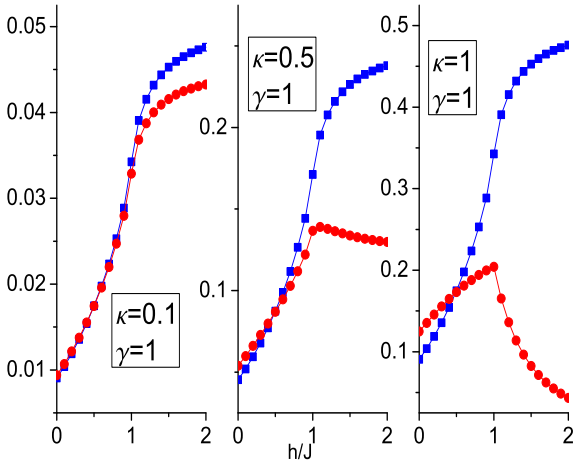

FIG. 7: Mean $\overline{m}/N$ (blue squares) and variance var/N (red circles) of the counting distribution of every second fermion as a function of $g = h/J$ for $\gamma = 1$, and indicated values of κ.

which is in the same form as in Eq. (19), with the product restricted, however, to $N/4-1$ terms. We then easily derive analogous recurrences as in the cases considered so far. Fig. 7 show the behavior of the mean and the variance, when counting every second spin, in the transverse Ising model. Note that the traces of singular behavior at $g = g_c$ persist. What is perhaps more interesting is that the general behavior is more rich. In particular, there is a crossing from sub- to super-possoinian behavior at $g = 0.5$. For $\gamma \to 0$ the point of crossing moves to zero, and the variance disappears.

IV. SUMMARY

Summarizing, we have formulated and applied fermion and spin counting theory to a family of one-dimensional strongly correlated systems that can be realized and detected with ultracold atoms. The counting distributions exhibit traces of singularities at criticality, that persist even at low detection efficiencies. They show various kinds of rich behavior, such as transitions from sub- to super-Poissonian character and even-odd oscillations.

Acknowledgments

We acknowledge support from the Spanish MEC (FIS-2005-04627, Consolider Ingenio 2010 QOIT, Acciones Integradas, & Ramón y Cajal), ESF Programmes QUDEDIS and Euroquam FERMIX, DAAD (German Academic Exchange Service), the Ministry of Education of the Generalitat de Catalunya, and EU IP SCALA.

[1] R.J. Glauber, in *Quantum Optics and Electronics*, eds. B. DeWitt, C. Blandin, and C. Cohen-Tannoudji, pp. 63-185 (Gordon and Breach, New York, 1965).

[2] M. Yasuda and F. Shimizu, Phys. Rev. Lett. **77**, 3090 (1996).

[3] M. Schellekens, R. Hoppeler, A. Perrin, J. Viana Gomes, D. Boiron, A. Aspect, and C.I. Westbrook, Science **310**, 648 (2005).

[4] T. Jeltes, J. M. McNamara, W. Hogervorst, W. Vassen, V. Krachmalnicoff, M. Schellekens, A. Perrin, H. Chang, D. Boiron, A. Aspect, and C. I. Westbrook, Nature **445**, 402 (2007).

[5] A. Öttl, S. Ritter, M. Köhl, and T. Esslinger, Phys. Rev. Lett. **95**, 090404 (2005).

[6] M. Lewenstein, Nature **445**, 372 (2007).

[7] J.L. Sørensen, J. Hald, and E.S. Polzik, Phys. Rev. Lett. **80**, 3847 (1998).

[8] K. Eckert, Ł. Zawitkowski, A. Sanpera, M. Lewenstein, and E. Polzik, Phys. Rev. Lett. **98**, 100404 (2007).

[9] K. Eckert, O. Romero-Isart, M. Rodriguez, M. Lewenstein, E.S. Polzik, and A. Sanpera, in print in Nature Physics (arXiv:0709.0527).

[10] S. Sachdev, *Quantum Phase Transitions* (CUP, Cambridge, 2001).

[11] R.W. Cherng and E. Demler, New J. Phys. **9**, 7 (2007).

[12] K.E. Cahill and R.J. Glauber, Phys. Rev. A **59** 1538 (1999).

[13] M. Lewenstein, L. Santos, M.A. Baranov, and H. Fehrmann, Phys. Rev. Lett. **92**, 050401 (2004).

[14] M. Lewenstein, A. Sanpera, V. Ahufinger, B. Damski, A. Sen(De), and U. Sen, Adv. in Phys. **56**, 243 (2007).

[15] U. Dorner, P. Fedichev, D. Jaksch, M. Lewenstein, and P. Zoller, Phys. Rev. Lett. **91**, 073601 (2003).

[16] J. Wehr, A. Niederberger, L. Sanchez-Palencia, and M. Lewenstein, Phys. Rev. B **74**, 224448 (2006).

[17] S. Katsura, Phys. Rev. **127**, 1508 (1962); P. Pfeuty, Ann. Phys. (N.Y.) **57**, 79 (1970); E. Lieb, T. Schultz, and D. Mattis, Ann. Phys. (N.Y.) **16**, 407 (1961); E. Barouch, B.M. McCoy and M. Dresden, Phys. Rev. A **2**, 1075 (1970); E. Barouch and B.M. McCoy, Phys. Rev. A **3**, 786 (1971); *ibid.*, 2137 (1971).

[18] I.S. Gradshteyn and I.M. Ryzhik, *Table of Integrals, Series, and Products*, (Academic Press, San Diego, 2000).